INTERNATIONAL JOURNAL FOR NUMERICAL METHODS IN FLUIDS, VOL. 9, 569–582 (1989)

A FINITE ELEMENT ANALYSIS OF A FREE SURFACE DRAINAGE PROBLEM OF TWO IMMISCIBLE FLUIDS

MASATAKE MORI AND MAKOTO NATORI

Institute of Information Sciences and Electronics, University of Tsukuba, Tsukuba, Ibaraki, 305, Japan

AND

ZHANG GUO-FENG*

Master's Program in Scientific Technology, University of Tsukuba, Tsukuba, Ibaraki, 305, Japan

SUMMARY

A sharp interface problem arising in the flow of two immiscible fluids, slag and molten metal in a blast furnace, is formulated using a two-dimensional model and solved numerically. This problem is a transient two-phase free or moving boundary problem, the slag surface and the slag–metal interface being the free boundaries. At each time step the hydraulic potential of each fluid satisfies the Laplace equation which is solved by the finite element method. The ordinary differential equations determining the motion of the free boundaries are treated using an implicit time-stepping scheme. The systems of linear equations obtained by discretization of the Laplace equations and the equations of motion of the free boundaries are incorporated into a large system of linear equations. At each time step the hydraulic potential in the interior domain and its derivatives on the free boundaries are obtained simultaneously by solving this linear system of equations. In addition, this solution directly gives the shape of the free boundaries at the next time step. The implicit scheme mentioned above enables us to get the solution without handling normal derivatives, which results in a good numerical solution of the present problem. A numerical example that simulates the flow in a blast furnace is given.

KEY WORDS Flow analysis Free surface problem Finite element method Blast furnace

A FREE SURFACE DRAINAGE PROBLEM

In this paper we consider a gravity drainage problem of slag and molten metal in a blast furnace and present a numerical method to solve it using the finite element method. Since slag and molten metal are immiscible with each other, the boundary between the slag and the metal forms a sharp interface, so that this flow problem can be formulated as a free or moving boundary problem, the slag surface and the slag–metal interface being the free boundaries.

The physical situation of the present problem is as follows. The hearth is packed with coke and the molten metal settles in the bottom of the hearth and the slag settles on it. It is assumed that initially the slag–metal interface is above the upper edge of the outlet. When the drainage is started from the outlet, the molten metal and the slag flow through the bed of coke towards the outlet. The molten metal drains out first, then both the molten metal and the slag drain out. The drainage process is terminated when the slag surface reaches the upper edge of the outlet because, if it is continued, gas at high temperature escapes from the outlet, which is very dangerous.

* Present address: Graduate School of Science and Technology, Kobe University, Rokkodai, Naka-ku, Kobe, 657, Japan.

0271–2091/89/050569–14$07.00

Received 6 November 1987
Revised 3 August 1988

In the present flow problem the coke plays the role of porous medium. There have been a variety of works on the numerical solution of sharp interface problems in porous media. Among other things, the governing equations and the interfacial boundary conditions of problems involving non-steady flow of groundwater and of interface problems between salt water and fresh water in a coastal aquifer are quite similar to those of the present problem. A typical approach to the flow problem through a dam was given by Neuman and Witherspoon[1] who used the finite element method. Also numerical solutions of the interface problem in a coastal aquifer were presented by Liu *et al.*[2] who used the boundary integral equation method. For other works see these papers and references therein. The boundary integral equation method or the boundary element method is known to be a powerful tool when solving such free boundary problems.[3] Also Crank[4] presented a good review of solutions of various free and moving boundary problems.

Natori and Kawarada solved a sharp interface problem of slag and molten metal numerically by the method of integrated penalty[5] and also by the boundary element method.[6] In a previous paper[7] we solved a one-phase problem in which only the slag exists by the finite element method. The purpose of the present paper is to solve the two-phase problem in which slag and molten metal exist by the finite element method and to compare the result with those obtained by the methods mentioned above.

As in the papers by Natori and Kawarada, we formulate the present problem in the form of a two-dimensional free boundary problem. For simplicity the side wall of the hearth is assumed to be perpendicular to the bottom, whose width is a as shown in Figure 1.

Let

$$y=f(x,t) \tag{1}$$

be the shape of the slag surface at time t and let

$$y=g(x,t) \tag{2}$$

be the shape of the slag–metal interface. These are the free boundaries to be determined. $D_1(t)$ and

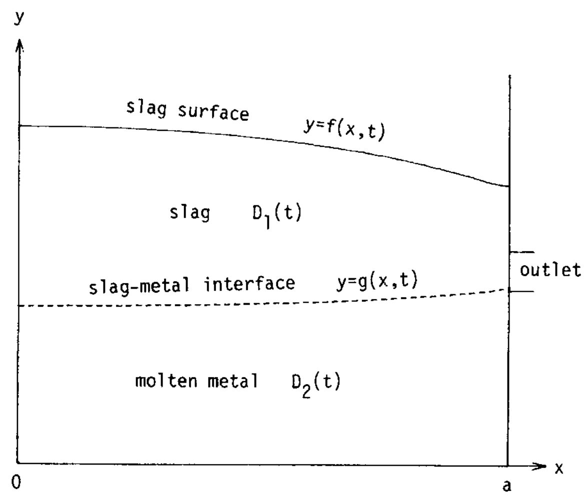

Figure 1. The domains $D_1(t)$ and $D_2(t)$ and the free boundaries

$D_2(t)$ denote the domains of the slag and the molten metal respectively:

$$D_1(t)=\{(x,y)|0<x<a,\ g(x,t)<y<f(x,t)\}, \tag{3}$$

$$D_2(t)=\{(x,y)|0<x<a,\ 0<y<g(x,y)\}. \tag{4}$$

The hydraulic potentials u_1 of the slag and u_2 of the molten metal are given by

$$u_1=\frac{p_1-p_0}{\gamma_1}+y \tag{5}$$

and

$$u_2=\frac{p_2-p_0}{\gamma_2}+y, \tag{6}$$

where y is the vertical height of each surface from the bottom, p_1 and p_2 are the pressures, p_0 is the pressure at the reference point and γ_1 and γ_2 are the specific weights in each domain. Since the slag and the molten metal flow through the bed of coke, i.e. through the porous medium, we can apply Darcy's law[3], and hence the velocities $\mathbf{v}_1$ and $\mathbf{v}_2$ of the slag and the molten metal are given by

$$\mathbf{v}_1=-K_1 \operatorname{grad} u_1, \tag{7}$$

$$\mathbf{v}_2=-K_2 \operatorname{grad} u_2, \tag{8}$$

where K_1 and K_2 are the hydraulic conductivities of the slag and the molten metal respectively, which are assumed to be constant. Substituting these equations into the equations of continuity

$$\operatorname{div} \mathbf{v}_1=0, \tag{9}$$

$$\operatorname{div} \mathbf{v}_2=0, \tag{10}$$

we have a pair of Laplace equations

$$\Delta u_1=0, \tag{11}$$

$$\Delta u_2=0 \tag{12}$$

for the hydraulic potentials in each domain.

Next we consider the boundary conditions for u_1 and u_2. Since the pressure is assumed to be constant p_0 on the slag surface, we have

$$u_1=f(x,t) \quad \text{on} \quad y=f(x,t). \tag{13}$$

On the slag–metal interface the pressure of the slag is equal to that of the molten metal, i.e.

$$p_1=p_2 \quad \text{on} \quad y=g(x,t).$$

We substitute this into (5) and (6) to give

$$u_1-\frac{\gamma_2}{\gamma_1}u_2=\left(1-\frac{\gamma_2}{\gamma_1}\right)g(x,t) \quad \text{on} \quad y=g(x,t). \tag{14}$$

Also, since the normal components of the fluid flux are equal to each other on the slag–metal interface, we have

$$K_1\frac{\partial u_1}{\partial n_1}=-K_2\frac{\partial u_2}{\partial n_2}, \tag{15}$$

where n_1 and n_2 are outward normals to the boundary of each domain. On the three impermeable walls $y=0$, $x=0$ and $x=a$ the normal component of the fluid flux is zero except on the outlet:

$$\frac{\partial u_1}{\partial n_1}=0, \tag{16}$$

$$\frac{\partial u_2}{\partial n_2}=0. \tag{17}$$

On the outlet we assume that the drainage rate is constant v_0:

$$\frac{\partial u_1}{\partial n_1}=-\frac{1}{K_1}v_0, \tag{18}$$

$$\frac{\partial u_2}{\partial n_2}=-\frac{1}{K_2}v_0. \tag{19}$$

Finally the motion of the slag surface $f(x,t)$ is determined by the standard kinematic boundary condition

$$\frac{\partial f}{\partial t}=-K_1\left[1+\left(\frac{\partial f}{\partial x}\right)^2\right]^{1/2}\left.\frac{\partial u_1}{\partial n_1}\right|_{y=f(x,t)}. \tag{20}$$

Similarly the motion of the slag–metal interface $g(x,t)$ is given by

$$\frac{\partial g}{\partial t}=-K_2\left[1+\left(\frac{\partial g}{\partial x}\right)^2\right]^{1/2}\left.\frac{\partial u_2}{\partial n_2}\right|_{y=g(x,t)}. \tag{21}$$

APPLICATION OF THE FINITE ELEMENT METHOD

Since our problem is a time-dependent free boundary problem, we first discretize the time t:

$$t_k=k\Delta t, \quad k=0, 1, 2, \ldots. \tag{22}$$

At every time step t_k we solve the Laplace equations (11) and (12) by means of the finite element method, and the free boundaries are updated at each time step by (20) and (21), each of which is approximated by an implicit scheme as will be described in the next section. As will be shown later, the solutions of the Laplace equations and the new position of the free boundaries are obtained simultaneously in our method.

In order to apply the finite element method, we divide the domain $D_1(t)$ and $D_2(t)$ into triangular elements as follows. First we subdivide the interval $(0,a)$ on the x-axis into m subintervals with nodal points

$$x_0(=0),\ x_1,\ x_2,\ \ldots,\ x_m(=a) \tag{23}$$

in such a way that the subinterval becomes smaller as it is closer to $x=a$. Next suppose that at $t=t_k$ the shape of the slag–metal interface $y=g(x,t_k)$ and that of the slag surface $y=f(x,t_k)$ are obtained. Then in $D_2(t)$ we subdivide the vertical line segment bounded by $(x_i,0)$ and $(x_i,g(x_i,t_k))$ into n_2 intervals, so that the width $h_i^{(2)}$ of the subinterval is given by

$$h_i^{(2)}=\frac{1}{n_2}g(x_i,t_k). \tag{24}$$

Therefore the nodal points in the domain $D_2(t_k)$ are

$$(x_i,\ jh_i^{(2)}), \quad j=0, 1, 2, \ldots, n_2. \tag{25}$$

Similarly in $D_1(t)$ we subdivide the vertical line segment bounded by $(x_i, f(x_i, t_k))$ and $(x_i, g(x_i, t_k))$ into n_1 equal subintervals with the width

$$h_i^{(1)} = \frac{1}{n_1}\,(f(x_i, t_k) - g(x_i, t_k)), \tag{26}$$

and hence the nodal points in the domain $D_1(t_k)$ are given by

$$(x_i, g(x_i, t_k) + jh_i^{(1)}), \quad j = 0, 1, 2, \ldots, n_1. \tag{27}$$

We number the nodal points from left to right and then from bottom to top as shown in Figure 2.

Table I shows to what quantity each of the nodal points is assigned. As seen in this table, each of the physical nodal points on the slag–metal interface is triply assigned, to u_2, to $\partial u_2/\partial n_2$ and to u_1. Also each of the physical nodal points on the slag surface is doubly assigned, to u_1 and to $\partial u_1/\partial n_1$.

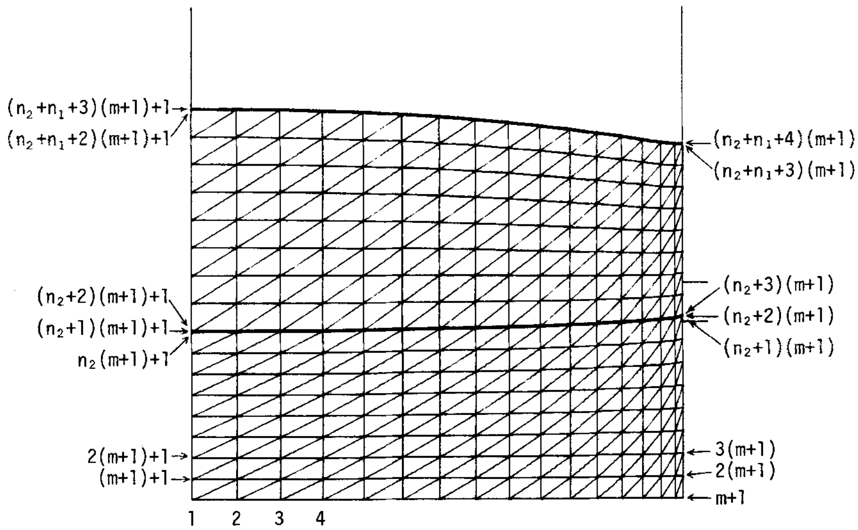

Figure 2. Triangulation of the domains for the finite element method and numbering of the nodal points

Table I. Assignment of the nodal points

Nodal points	Assigned to
$1 \sim n_2(m+1)$	u_2 in $D_2(t)$
$n_2(m+1)+1 \sim (n_2+1)(m+1)$	u_2 on the slag–metal interface
$(n_2+1)(m+1)+1 \sim (n_2+2)(m+1)$	$\partial u_2/\partial n_2$ on the slag–metal interface
$(n_2+2)(m+1)+1 \sim (n_2+3)(m+1)$	u_1 on the slag–metal interface
$(n_2+3)(m+1)+1 \sim (n_2+n_1+2)(m+1)$	u_1 in $D_1(t)$
$(n_2+n_1+2)(m+1)+1 \sim (n_2+n_1+3)(m+1)$	u_1 on the slag surface
$(n_2+n_1+3)(m+1)+1 \sim (n_2+n_1+4)(m+1)$	$\partial u_1/\partial n_1$ on the slag surface

Let $\phi_j(x,y)$ be the piecewise linear function which takes the value one at the jth node and vanishes at other nodes. $\phi_j(x,y)$ is assumed to be identically zero outside the domain. We expand the approximate solution $\tilde{u}_1$ to u_1 in the domain $D_1(t_k)$ in terms of $\{\phi_j\}$:

$$\tilde{u}_1(x,y)=\sum_{j=(n_2+2)(m+1)+1}^{(n_2+n_1+3)(m+1)} u_j\phi_j(x,y). \tag{28}$$

Similarly we expand the approximate solution $\tilde{u}_2$ to u_2 in the domain $D_2(t_k)$:

$$\tilde{u}_2(x,y)=\sum_{j=1}^{(n_2+1)(m+1)} u_j\phi_j(x,y). \tag{29}$$

The coefficient u_j is numbered consistently with the numbering of the nodal points. Note that the time t_k is not explicitly written in $\phi_j(x,y)$, $\tilde{u}_1(x,y)$ and $\tilde{u}_2(x,y)$ because we fix the time t_k when we solve the Laplace equations by the finite element method.

We temporarily separate the present problem into two problems; one is in the domain $D_1(t_k)$ and the other is in the domain $D_2(t_k)$. Also we temporarily assume that the normal derivative on the slag surface is specified as a given boundary value $q^{(0)}(x,t_k)$ and those on the slag–metal interface as $q^{(1)}(x,t_k)$ in $D_1(t_k)$ and $q^{(2)}(x,t_k)$ in $D_2(t_k)$, although they are actually unknowns. Then the problems become as follows. For the slag domain:

$$\Delta u_1=0 \quad \text{in} \quad D_1(t_k), \tag{30}$$

$$\frac{\partial u_1}{\partial n_1}=0 \quad \text{on} \quad x=0 \text{ and } x=a \text{ (except on the outlet)}, \tag{31}$$

$$\frac{\partial u_1}{\partial n_1}=-\frac{1}{K_1}v_0 \quad \text{on the outlet}, \tag{32}$$

$$\frac{\partial u_1}{\partial n_1}=q^{(0)}(x,t_k) \quad \text{on the slag surface}, \tag{33}$$

$$\frac{\partial u_1}{\partial n_1}=q^{(1)}(x,t_k) \quad \text{on the slag–metal interface}. \tag{34}$$

For the molten metal domain:

$$\Delta u_2=0 \quad \text{in} \quad D_2(t_k), \tag{35}$$

$$\frac{\partial u_2}{\partial n_2}=0 \quad \text{on} \quad y=0,\ x=0,\ x=a \text{ (except on the outlet)}, \tag{36}$$

$$\frac{\partial u_2}{\partial n_2}=-\frac{1}{K_2}v_0 \quad \text{on the outlet}, \tag{37}$$

$$\frac{\partial u_2}{\partial n_2}=q^{(2)}(x,t_k) \quad \text{on the slag–metal interface}. \tag{38}$$

Now we apply the finite element method using (28) and (29) to obtain two systems of linear equations for the slag domain and for the molten metal domain. Here we assumed that in the neighbourhood of the $((n_2+1)(m+1)+i)$th nodal point on the slag–metal interface $q^{(2)}(x,t_k)$ is approximately equal to a constant $q^{(2)}_{(n_2+1)(m+1)+i}=q^{(2)}(x_i,t_k)$ and moved it outside the integral. Also we make the same assumption on $q^{(1)}(x,t_k)$ and $q^{(0)}(x,t_k)$. Next we regard $q_j^{(0)}$, $q_j^{(1)}$ and $q_j^{(2)}$ as unknowns and move the terms including $q_j^{(0)}$, $q_j^{(1)}$ and $q_j^{(2)}$ to the left-hand side of the equations.

Thus, for the molten metal domain, we obtain a system of linear equations

$$\overbrace{\hphantom{\mathbf{K}^{(2)}}}^{(n_2+1)(m+1)}\ \overbrace{\hphantom{0}}^{m+1}$$

$$(n_2+1)(m+1)\left\{\begin{bmatrix} \mathbf{K}^{(2)} & \begin{matrix} \mathbf{0} \\ \cdots \\ \mathbf{B}^{(2)} \end{matrix} \end{bmatrix}\right.\begin{bmatrix} \mathbf{u}^{(2)} \\ \cdots \\ \mathbf{q}^{(2)} \end{bmatrix}=\begin{bmatrix} \mathbf{v}^{(2)} \\ \cdots \\ \mathbf{0} \end{bmatrix}, \tag{39}$$

where $\mathbf{u}^{(2)}$ is a vector whose components are u_j, $j=1, 2, \ldots, (n_2+1)(m+1)$ and $\mathbf{q}^{(2)}$ is a vector whose components are $q_j^{(2)}$, $j=(n_2+1)(m+1)+1, \ldots, (n_2+2)(m+1)$. $\mathbf{K}^{(2)}$ is an $(n_2+1)(\mathrm{m}+1)\times(n_2+1)(m+1)$ stiffness matrix whose (i, j) component is given by

$$K_{ij}^{(2)}=\iint_{D_2(t_k)}\left(\frac{\partial\phi_i}{\partial x}\frac{\partial\phi_j}{\partial x}+\frac{\partial\phi_i}{\partial y}\frac{\partial\phi_j}{\partial y}\right)\mathrm{d}x\mathrm{d}y. \tag{40}$$

$\mathbf{B}^{(2)}$ is an $(m+1)\times(m+1)$ diagonal matrix whose (i,i) component is given by

$$B_{ii}^{(2)}=-\int_{\text{interface}}\phi_i\mathrm{d}\sigma. \tag{41}$$

The line integral is along the slag–metal interface. $\mathbf{v}^{(2)}$ on the right-hand side of (39) is a vector whose ith component is

$$-\frac{v_0}{K_2}\int_{\text{outlet}}\phi_i\mathrm{d}\sigma. \tag{42}$$

The line integral is along the outlet. This integral vanishes unless the nodal point i is located on the outlet or on the wall adjacent to it.

Similarly we have the following system of linear equations of the slag domain:

$$\overbrace{\hphantom{B}}^{m+1}\ \overbrace{\hphantom{\mathbf{K}^{(1)}}}^{(n_1+1)(m+1)}\ \overbrace{\hphantom{0}}^{m+1}$$

$$(n_1+1)(m+1)\left\{\begin{bmatrix} \begin{matrix} \mathbf{B}^{(1)} \\ \cdots \\ \\ \mathbf{0} \end{matrix} & \mathbf{K}^{(1)} & \begin{matrix} \\ \mathbf{0} \\ \cdots \\ \mathbf{B}^{(0)} \end{matrix} \end{bmatrix}\right.\begin{bmatrix} \mathbf{q}^{(2)} \\ \cdots \\ \mathbf{u}^{(1)} \\ \cdots \\ \mathbf{q}^{(0)} \end{bmatrix}=\begin{bmatrix} \mathbf{0} \\ \cdots \\ \mathbf{v}^{(1)} \\ \cdots \\ \mathbf{0} \end{bmatrix}. \tag{43}$$

Here we used

$$\frac{\partial u_1}{\partial n_1}=-\frac{K_2}{K_1}q^{(2)}(x,t)$$

instead of (34) in view of (15). $\mathbf{u}^{(1)}$ is a vector whose components are $u_j, j=(n_2+2)(m+1)+1, \ldots, (n_2+n_1+3)(m+1)$ and $\mathbf{q}^{(0)}$ is a vector whose components are $q_j^{(0)}, j=(n_2+n_1+3)(m+1)+1, \ldots, (n_2+n_1+4)(m+1)$. $\mathbf{K}^{(1)}$ is an $(n_1+1)(m+1)\times(n_1+1)(m+1)$ stiffness matrix whose (i, j) component is given by

$$K_{ij}^{(1)}=\iint_{D_1(t_k)}\left(\frac{\partial\phi_i}{\partial x}\frac{\partial\phi_j}{\partial x}+\frac{\partial\phi_i}{\partial y}\frac{\partial\phi_j}{\partial y}\right)\mathrm{d}x\mathrm{d}y. \tag{44}$$

$\mathbf{B}^{(1)}$ and $\mathbf{B}^{(0)}$ are $(m+1)\times(m+1)$ diagonal matrices whose (i,i) components are given by

$$B_{ii}^{(1)}=\frac{K_2}{K_1}\int_{\text{interface}}\phi_i\mathrm{d}\sigma \tag{45}$$

and

$$B_{ii}^{(0)} = -\int_{\text{slag surface}} \phi_i \mathrm{d}\sigma \tag{46}$$

respectively. The line integral in (46) is along the slag surface. $\mathbf{v}^{(1)}$ on the right-hand side of (43) is a vector whose ith component is

$$-\frac{v_0}{K_1}\int_{\text{outlet}} \phi_i \mathrm{d}\sigma . \tag{47}$$

As in the case of $\mathbf{v}^{(2)}$, this integral vanishes unless the node i is located on the outlet or on the wall adjacent to it.

DISCRETIZATION OF THE EQUATIONS FOR THE FREE SURFACES

Each of the coefficient matrices of the system of equations (39) and (43) is of course singular because only natural boundary conditions are specified. In this section we assemble these equations together with (20) and (21) to construct a system which has a relevant solution.

Note that the hydraulic conductivity of the molten metal is much larger than that of the slag, i.e. $K_2 \gg K_1$. Therefore, by physical intuition, we see that in the initial stage of the drainage the major part of the fluid that drains out is the molten metal and that the slag–metal interface falls fast and its right edge comes close to the lower edge of the outlet in a relatively small time interval. However, after that, the major part of the fluid that drains out is the slag and the speed of fall of the slag–metal interface becomes very slow. In other words, the motion of the slag–metal interface has a component with a time constant which is very small relative to the interval of the entire process of drainage. Thus the full system of the differential equations (20) and (21) together with (39) and (43) is essentially stiff. Therefore it is obvious that we cannot obtain a stable solution if we use an explicit scheme for (20) and (21).

For this reason we employ an implicit scheme for (20) and (21) as follows. We approximate the left-hand side of (20) by the finite difference

$$\frac{\partial f}{\partial t} \fallingdotseq \frac{f(x_i, t_k) - f(x_i, t_{k-1})}{\Delta t}. \tag{48}$$

On the other hand, we use the value at $t = t_k$ for $\partial u_1/\partial n_1|_{y=f(x,t)}$ in the right-hand side of (20). This results in an implicit scheme and causes the stability of the scheme for a fairly large Δt. For $\partial f/\partial x$ appearing in the square root in the right-hand side of (20) we use the value at $t = t_{k-1}$ in order to preserve linearity with respect to the values at $t = t_k$. Thus we have

$$f(x_i, t_k) = f(x_i, t_{k-1}) - K_1 \Delta t \left[1 + \left(\frac{\partial f(x_i, t_{k-1})}{\partial x} \right)^2 \right]^{1/2} q^{(0)}(x_i, t_k) \tag{49}$$

in which we replaced $\partial u_1/\partial n_1|_{y=f(x,t_k)}$ with $q^{(0)}$ in view of (33). The derivative $\partial f(x_i, t_{k-1})/\partial x$ is approximated by the finite difference scheme

$$\frac{h}{h+k}\frac{f(x_{i+1}) - f(x_i)}{k} - \frac{k}{h+k}\frac{f(x_i) - f(x_{i-1})}{h} + O(hk),$$

$$h = x_i - x_{i-1}, \qquad k = x_{i+1} - x_i. \tag{50}$$

In view of (13) we put in the left-hand side of (49)

$$f(x_i, t_k) = u_1(x_i, f(x_i, t_k), t_k) \fallingdotseq \tilde{u}_1(x_i, f(x_i, t_k)) = u_{j-m-1}, \tag{51}$$

so that we have

$$u_{j-m-1}+K_1\Delta t\left[1+\left(\frac{\partial f(x_i,t_{k-1})}{\partial x}\right)^2\right]^{1/2} q_j^{(0)}=f(x_i,t_{k-1}),$$
$$j=(n_2+n_1+3)\,(m+1)+1,\ldots,(n_2+n_1+4)\,(m+1) \tag{52}$$

on the slag surface.

Similarly from (21) and (38) we have

$$g(x_i,t_k)=g(x_i,t_{k-1})-K_2\Delta t\left[1+\left(\frac{\partial g(x_i,t_{k-1})}{\partial x}\right)^2\right]^{1/2} q^{(2)}(x_i,t_k) \tag{53}$$

on the slag–metal interface. We also approximate $\partial g(x_i,t_{k-1})/\partial x$ by a finite difference scheme similar to (50). We multiply by $1-\gamma_2/\gamma_1$ on both sides of (53) and put

$$\left(1-\frac{\gamma_2}{\gamma_1}\right) g(x_i,t_k)=u_1-\frac{\gamma_2}{\gamma_1}u_2\doteq\tilde{u}_1(x_i,g(x_i,t_k))-\frac{\gamma_2}{\gamma_1}\,\tilde{u}_2(x_i,g(x_i,t_k))=u_{j+m+1}-\frac{\gamma_2}{\gamma_1}\,u_{j-m-1} \tag{54}$$

in view of (14). Then we have

$$u_{j+m+1}-\frac{\gamma_2}{\gamma_1}\,u_{j-m-1}+\left(1-\frac{\gamma_2}{\gamma_1}\right)K_2\Delta t\left[1+\left(\frac{\partial g(x_i,t_{k-1})}{\partial x}\right)^2\right]^{1/2} q_j^{(2)}$$
$$=\left(1-\frac{\gamma_2}{\gamma_1}\right)g(x_i,t_{k-1}),\quad j=(n_2+1)\,(m+1)+1,\ldots,(n_2+2)\,(m+1) \tag{55}$$

on the slag–metal interface.

Finally we incorporate (39), (55), (43) and (52) to obtain a full system of $(n_2+n_1+4)\,(m+1)$ linear equations as shown in Figure 3. In Figure 3 $\mathbf{D}^{(2)}$ and $\mathbf{D}^{(0)}$ are $(m+1)\times(m+1)$ diagonal matrices whose (i,i) components are given by

$$D_{ii}^{(2)}=\left(1-\frac{\gamma_2}{\gamma_1}\right)K_2\Delta t\left[1+\left(\frac{\partial g(x_i,t_{k-1})}{\partial x}\right)^2\right]^{1/2} \tag{56}$$

and

$$D_{ii}^{(0)}=K_1\Delta t\left[1+\left(\frac{\partial f(x_i,t_{k-1})}{\partial x}\right)^2\right]^{1/2} \tag{57}$$

respectively. $\mathbf{I}$ is the identity matrix. $\mathbf{g}$ and $\mathbf{f}$ are vectors whose ith components are

$$g_i=\left(1-\frac{\gamma_2}{\gamma_1}\right) g(x_i,t_{k-1}) \tag{58}$$

and

$$f_i=f(x_i,t_{k-1}), \tag{59}$$

respectively. The hydraulic potential and its derivatives on the free surfaces are obtained simultaneously by solving this full system of equations. This resembles very much the situation encountered in the boundary element method.

Also note that the new position of the slag–metal interface $f(x_i,t_k)$ and that of the slag–metal interface $g(x_i,t_k)$ are obtained immediately from the solution using the relations (51) and (54), and that, accordingly, we do not use the normal derivatives at all throughout the computation.

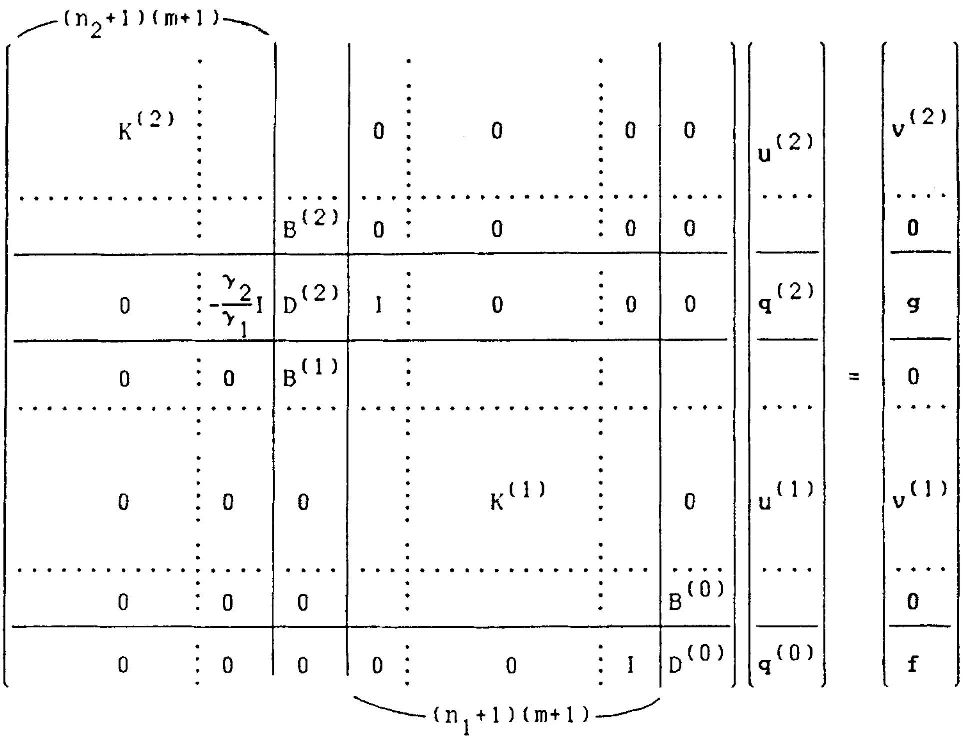

Figure 3. The matrix equation to be solved

Although the system of equations shown in Figure 3 is not symmetric, we can symmetrize it by the following procedure:

(i) Multiply $(\gamma_1/\gamma_2)\int_{\text{interface}}\phi_j d\sigma$ by the equation (55) corresponding to the jth nodal point; this makes the components in the transposed position of $\mathbf{B}^{(2)}$ equal to $\mathbf{B}^{(2)}$ itself in (39).

(ii) Next multiply $(\gamma_1/\gamma_2)\times(K_1/K_2)$ by each of the equations in (43); this makes the components in the transposed position of $\mathbf{B}^{(1)}$ equal to $\mathbf{B}^{(1)}$ itself in (43).

(iii) Finally multiply $-(\gamma_1/\gamma_2)\times(K_1/K_2)\int_{\text{slag surface}}\phi_j d\sigma$ by the equation (52) corresponding to the jth nodal point; this makes the components in the transposed position of $\mathbf{B}^{(0)}$ equal to $\mathbf{B}^{(0)}$ itself in (43).

Thus we obtain a symmetric system of $(n_2+n_1+4)(m+1)$ equations. Since it is symmetric and sparse it can be solved efficiently by the ICCG (incomplete Cholesky decomposition conjugate gradient) method.[8-10]

In solving a similar non-steady interface problem to ours, one usually solves the system of linear equations obtained, say, by the finite element method at each time step and then updates the boundary using some relation independent of the system of linear equations. In other words, the potential in the interior domain and the new position of the free boundary are computed sequentially. In our method, on the other hand, these two quantities are computed simultaneously as stated above only through the solution of the system of $(n_2+n_1+4)(m+1)$ equations. When we get the new position of the free boundaries $f(x_i, t_k)$ and $g(x_i, t_k)$, additional calculation is not necessary except (54). Using the updated $f(x_i, t_k)$ and $g(x_i, t_k)$ we subdivide the domains $D_1(t_k)$ and $D_2(t_k)$ and proceed to the next time step.

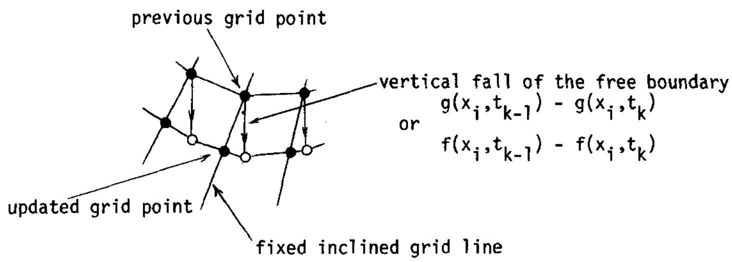

Figure 4. Interpolation of the vertical fall of the free boundary for the inclined side wall geometry

In short, the present method is characterized by the following two strategies. The first one is that we temporarily introduced the natural boundary conditions (33), (34) and (38), and the second one is that we employed an implicit approximation to (20) and (21). The incorporation of these two strategies enables us to get the solution without handling the normal derivatives explicitly so that we can avoid deterioration of the accuracy of computation due to this handling.

In the present paper we assumed for simplicity that the side wall of the hearth is perpendicular to the bottom because the side wall of the bed of the real hearth is approximately perpendicular to the bottom. Our scheme, however, may be extended to one which deals with the inclined side wall if we replace the fixed vertical grid lines in Figure 2 with fixed inclined grid lines and, at each time step, subdivide each inclined grid line segment bounded by, say, the bottom wall and the slag–metal interface in order to update the grid points for the finite element triangulation. Since we employ the finite element method, it does not matter whether the triangles are right-angled or not. The only point to be noted is that when the side wall is inclined, the updated position of the free boundary on each fixed inclined grid line is obtained by the interpolation of its vertical fall $g(x_i, t_{k-1}) - g(x_i, t_k)$ or $f(x_i, t_{k-1}) - f(x_i, t_k)$ as shown in Figure 4.

A NUMERICAL EXAMPLE AND DISCUSSION

In this section we show the result of a numerical experiment. The physical parameters we choose here are the same as those chosen by Natori and Kawarada[6] and Mori and Natori[7] which simulate a real situation in the blast furnace:

$$\begin{aligned} &a=1, \quad K_1=7{\cdot}5, \quad K_2=1875, \quad \gamma_2/\gamma_1=4{\cdot}1875, \\ &\text{outlet:} \quad x=a=1, \quad 0{\cdot}09 \leqslant y \leqslant 0{\cdot}11. \end{aligned} \tag{60}$$

The initial condition is

$$\begin{aligned} f(x,0)&=0{\cdot}25, \\ g(x,0)&=0{\cdot}12 \end{aligned} \tag{61}$$

and the drainage rate is

$$v_0 = 2{\cdot}25. \tag{62}$$

In order to apply the finite element method we divide $(0, a)$ on the bottom by

$$x_i = a\left\{1 - \left(\frac{m-i}{m-1}\right)^{1{\cdot}5}\right\}, \quad i=1, 2, \ldots, m, \quad m=16, \tag{63}$$

and choose

$$\begin{aligned} n_1 &= 8 \quad \text{in } D_1, \\ n_2 &= 8 \quad \text{in } D_2. \end{aligned} \tag{64}$$

For the time mesh we take

$$\Delta t = 0{\cdot}16 \tag{65}$$

and the computation is terminated when the slag surface reaches the upper edge of the outlet.

As already mentioned, the system of linear equations at each time step was solved by the ICCG method in which the incomplete Cholesky decomposition $\mathbf{LDL}^{\mathrm{T}}$ is such that we neglect the component of $\mathbf{L}$ if the component in the same position of the original matrix is zero.

The change of the slag surface and the slag–metal interface is shown in Figure 5. This agrees quite well with the result obtained by Mori and Natori[7] using the boundary element method. Unfortunately we cannot compare our result with the actual flow in the blast furnace because, as far as we know, there have been no experimental data observed in the blast furnace. The only physical simulation is given by Pinczeski *et al.*[11] in which glycerol and mercury were used instead of slag and molten metal. Their result is qualitatively similar to ours.

We mentioned that our present scheme is stable for a fairly large Δt because we use an implicit scheme. In fact our scheme was completely stable with $\Delta t = 0{\cdot}32$ and gave almost the same solution as in the case with $\Delta t = 0{\cdot}16$.[12] We did not find significant differences between the plots of the free boundaries with $\Delta t = 0{\cdot}32$ and $\Delta t = 0{\cdot}16$ in Figure 5 except a very small one in the close neighbourhood of the outlet.

As a measure of the accuracy of computation we computed

$$\varepsilon = \left| \frac{V_0 - V_s}{V_0} \right|, \tag{66}$$

where V_s is the decrease per Δt of the area of the domain $D_1 + D_2$ due to the fall of the slag surface and $V_0 = \Delta t \times v_0 \times$ (radius of the outlet) is the volume of the fluid drained per Δt from the outlet. Although in the initial stage of drainage ε is as small as about 10^{-7}, it becomes about 5×10^{-5} as the slag surface approaches the outlet, and the average value of ε is $1{\cdot}3 \times 10^{-5}$.

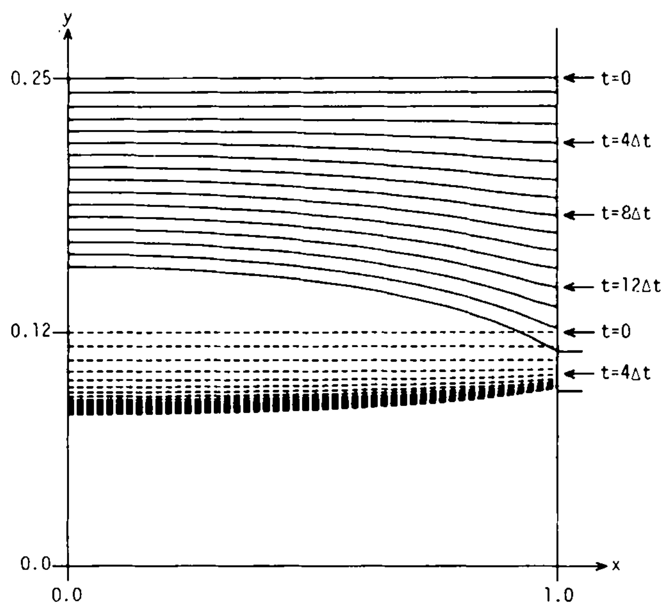

Figure 5. Change of the slag surface (solid curves) and the slag–metal interface (dotted curves)

The velocity vectors at $t = 4\Delta t = 0{\cdot}64$ and $t = 8\Delta t = 1{\cdot}28$ computed from the hydraulic potential are shown in Figures 6 and 7 respectively. Before around $t = 4\Delta t$ mainly the molten metal drains out, but after around this time step the slag becomes the major part of the fluid that drains out and the molten metal drains very little. In the present numerical experiment an interesting

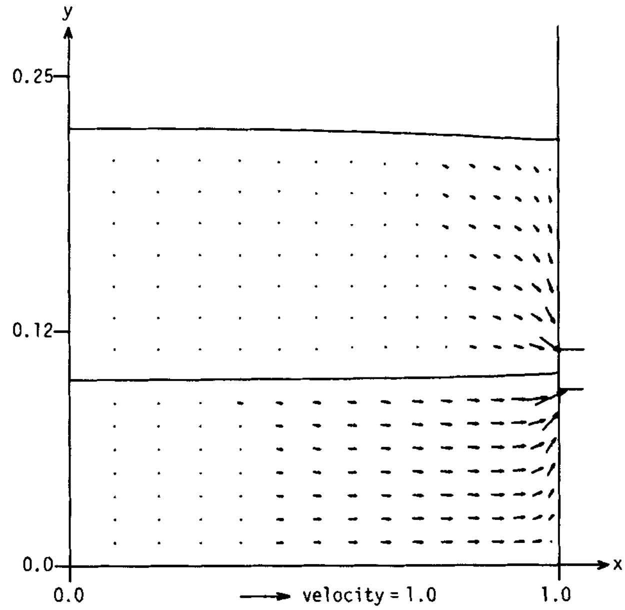

Figure 6. Velocity vectors at $t = 4\Delta t = 0{\cdot}64$

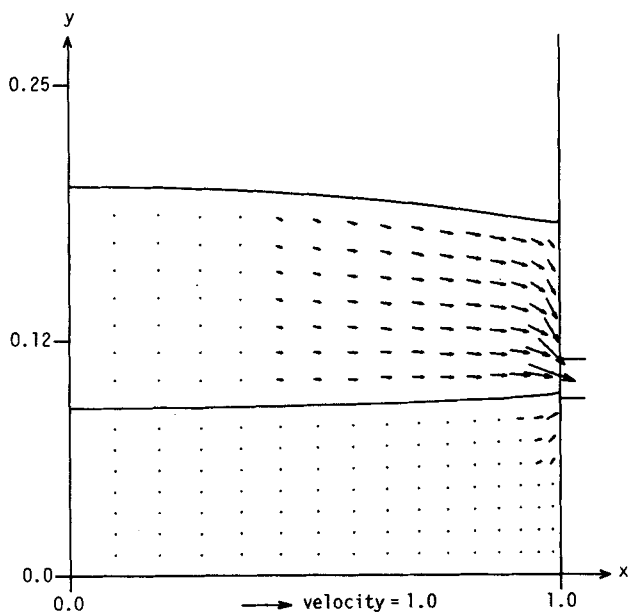

Figure 7. Velocity vectors at $t = 8\Delta t = 1{\cdot}28$

phenomenon is observed, as reported in the physical simulation by Pinczeski et al.[11] mentioned above, that the molten metal continues to drain, although very little, even after the average slag-metal interface has become substantially lower than the lower edge of the outlet as seen in Figure 7. It is also observed in our numerical experiment that at the final stage of the drainage the slag-metal interface ascended in the very close neighbourhood of the outlet.

The CPU time necessary for the present computation using the finite element mehod was compared with that necessary for the computation using the boundary element method by Natori and Kawarada[6] and Mori and Natori[7] with nearly the same number of nodal points on the boundary in the same computer environment. It turned out that the CPU time by the finite element method was about half of that by the boundary element method. The ICCG method for the present sparse symmetric matrix equation plays a significant role in reducing the CPU time. The higher efficiency of the finite element method than that of the boundary element method in some problems similar to ours has also been reported,[13] although the method to solve the system of linear equations is not explicitly mentioned there. In addition, in the present computation by the finite element method the hydraulic potential in the interior domain is obtained as a byproduct, while in the computation by the boundary element method much additional CPU time becomes necessary if the potential in the interior domain is required. Therefore we conclude that, to solve the present two-phase free boundary problem, the method presented here based on the finite element method is superior to the method based on the boundary element method.

ACKNOWLEDGEMENTS

The authors are indebted to the referees for bringing several related papers to their notice.

REFERENCES

1. S. P. Neuman and P. A. Witherspoon, 'Analysis of nonsteady flow with a free surface using the finite element method', *Water Resources Res.*, **7**, 611–610 (1971).
2. P. L.-F. Liu, A. H.-D. Cheng and J. A. Liggett, "Boundary integral equation solutions to moving interface between two fluids in porous media', *Water Resources Res.*, **17**, 1445–1452 (1981).
3. J. A. Liggett and P. L.-F. Liu, *The Boundary Integral Equation Method for Porous Media Flow*, George Allen & Unwin, 1983.
4. J. Crank, *Free and Moving Boundary Problems*, Oxford Science Publications, Clarendon Press, 1984.
5. M. Natori and H. Kawarada, 'Numerical solution of free boundary problem for unsteady slag flow in the hearth', *Japan. J. Appl. Math.*, **2**, 187–196 (1985).
6. M. Natori and H. Kawarada, 'Numerical solution of the free surface drainage problem of two immiscible fluids by the boundary element method', *Japan. J. Appl. Phys.*, **24**, 1363–1366 (1985).
7. M. Mori and M. Natori, 'FEM and BEM applied to a free boundary problem for flows in a blast furnace', in R. Glowinski and J.-L. Lions (eds), *Computing Methods in Applied Sciences and Engineering VII*, North-Holland, 1986, pp. 275–286.
8. A. Meijerink and H. A. van der Vorst, 'An iterative solution method for linear equation systems of which the coefficient matrix is a symmetric M-matrix', *Math. Comput.*, **31**, 148–162 (1977).
9. G. H. Golub and C. F. Van Loan, *Matrix Computations*, The Johns Hopkins University Press, 1983.
10. O. Axelsson and V. A. Barker, *Finite Element Solution of Boundary Value Problems*, Academic Press, 1984.
11. W. V. Pinczeski, W. B. U. Tanzil, M. I. Hoschke and J. M. Burgess, 'Simulation of the drainage of two liquids from a blast furnace hearth', *Tetsu-to-Hagane*, **68**, S111 (1982).
12. Zhang Guo-feng, A finite element analysis of a free boundary problem arising in a blast furnace (in Japanese), *Master Thesis*, University of Tsukuba, 1986.
13. E. C. Hume III, R. A. Brown and W. M. Deen, 'Comparison of boundary and finite element methods for moving-boundary problems governed by a potential', *Int. j. numer. methods eng.*, **21**, 1295–1314 (1985).